Applied Water Science (2022) 12:140
https://doi.org/10.1007/s13201-022-01668-6

ORIGINAL ARTICLE

Synthesis of CuAl-layered double hydroxide/MgO_2 nanocomposite catalyst for the degradation of organic dye under dark condition

Setegn Geta Aragaw[1] · Gebisa Bekele Feysia[1] · Noto Susanto Gultom[2] · Dong-Hau Kuo[2] · Hairus Abdullah[2] · Xiaoyun Chen[3] · Osman Ahmed Zelekew[1]

Received: 4 January 2022 / Accepted: 29 March 2022 / Published online: 22 April 2022

Abstract

Water pollution as a result of releasing organic and inorganic pollutants is the main concern and health risk factor for human beings. To minimize the effect of toxicity from pollutants, enormous method has been applied. In this report, the CuAl-layered double hydroxide/MgO_2 composite catalysts were synthesized via in-situ growth of magnesium peroxide on the layered double hydroxide (LDH) sheet. The preparations of the catalysts were performed with varying the ratio of LDH: MgO_2 which was abbreviated as CuAl-LDH/MgO_2-35, CuAl-LDH/MgO_2-50, and CuAl-LDH/MgO_2-65 for 35:65, 50:50, and 65:35% weight ratios, respectively. The prepared catalysts were characterized and evaluated for methyl orange (MO) dye degradation at room temperature under dark conditions. Among the catalysts, CuAl-LDH/MgO_2-50 showed an excellent Fenton-like reaction under neutral condition at which 97% of MO was degraded in the 100 min reaction. However, CuAl-LDH, MgO_2, CuAl-LDH/MgO_2-35, and CuAl-LDH/MgO_2-65 catalysts degrade only 61, 8, 35, and 69% of MO dye. The highest degradation efficiency for CuAl-LDH/MgO_2-50 could be due to the presence of optimum amount of copper along with the sufficient amount of generated hydrogen peroxide from MgO_2 to run the Fenton-like reaction process. Moreover, the catalyst can also be able to use repeatedly with a minimum loss of activity. In general, the result suggests that CuAl-LDH/MgO_2 composite is an option for the degradation of organic pollutants.

Keywords Fenton-like reaction · Layered double hydroxide · MgO_2 · Catalyst · Organic pollutants

Introduction

Organic pollutants such as phenols, pesticides, dyes, and other organic pollutants are a major threat for living things (Dvininov et al. 2010; Zelekew and Kuo 2017a). Since the developments of industries utilize several chemicals as input, effects related to effluents becomes worse recently (Lu et al. 2019). Particularly, chemicals released from industries and population growth are the main causes of water pollution and have led to an adverse effect on healthy life (Rupa et al. 2019). Therefore, the decontamination of polluted water resources is now the main concern for researchers around the globe (Zelekew et al. 2021). Although several water treatment methods such as filtration (Cardenas et al. 2016), sedimentation (Soltani et al. 2016), and distillation (Mustapha et al. 2020) were used, they have their own drawback in the complete removal of pollutants. Other methods such as adsorption and photocatalytic degradation have been used for wastewater treatment (Garcia-Muñoz et al. 2020; Wan et al. 2018). It is also reported that photocatalysis is an effective and efficient method for the treatment of wastewater (Opoku et al. 2017; Zhang et al. 2019). For this purpose, metal oxide catalysts can be used due to their efficiency, economical, and stability (Zelekew et al. 2017).

Metal oxides such as TiO_2 and ZnO are an important class of materials and are used for wastewater treatment (Ahmad et al. 2020; Marinho et al. 2017). However, they have their own limitations such as high electron and hole recombination rate and large bandgap (Opoku et al. 2017; Aragaw et al. 2020). To enhance the catalytic activities of metal oxide,

✉ Osman Ahmed Zelekew
osmanx2007@gmail.com; osman.ahmed@astu.edu.et

[1] Department of Materials Science and Engineering, Adama Science and Technology University, Adama, Ethiopia

[2] Department of Materials Science and Engineering, National Taiwan University of Science and Technology, Taipei 10607, Taiwan

[3] College of Materials Engineering, Fujian Agriculture and Forestry University, Fuzhou 350002, China

supporting materials to minimize agglomeration effects can be used (Zelekew and Kuo 2017b). In this perspective, layered materials and clays have been used as a support that can help to immobilize metal oxides and reduce agglomeration thereby providing a site for growth (Fei et al. 2019; Hadjltaief et al. 2021). Additionally, the layered double hydroxides (LDHs) which are synthetic anionic clay-like layered materials have been studied to treat pollutants through both adsorption and degradation process owing to their layered and special memorial property than the usually known metal oxides (Lu et al. 2016; Ali et al. 2020; Seftel et al. 2014).

It has been also reported that the Fenton-like advanced oxidation process is a promising technique for the prompting of strong oxidants even in a dark environment (Brillas and Garcia-Segura 2020). Particularly, iron has advantages due to plentiful abundance, low cost, adaptability to the environment, and being low-poisonous. However, the iron-based Fenton reactions required acidic condition, a cause for H_2O_2 transportation difficulties, and lead to lower lifetime in the oxidation reaction (Bokare and Choi 2014; Wu et al. 2019). Thus, many researchers have been engaged in the modification to cure the challenges present in conventional Fenton processes. Among the findings, using non-ferrous-based catalysts and in-situ generation of peroxide have been reported and showed an intensified performance (Asghar et al. 2015; Torres-Pinto et al. 2020). Latterly, metal peroxides exhibited much attention since these materials are economically advisable besides generating sufficient hydrogen peroxide (Wu et al. 2019). Such findings not only broaden Fenton-like activity to a wider pH range but also minimize the loss of catalysts that happened through precipitation. Particularly, Cu-based catalysts in Fenton-like reactions can provide great potential in Fenton reactions in which it can works in the neutral pH conditions unlike iron-based Fenton reactions (Ma et al. 2019).

It is also know that the LDH materials alone are not sufficient in the removal of pollutants due to the relatively lower charge transfer efficiency and the higher photo-generated electron and hole pairs recombination rate (Gao et al. 2021). Hence, combining the LDH with other materials such as oxides (Fei et al. 2019; Zhang et al. 2021), metals (Lestari et al. 2021), MOFs (Soltani et al. 2021), and rGO (Khataee et al. 2019) are important. In addition to LDH-based materials, peroxides are used in the degradation of pollutants due to their effectiveness with increasing the photogenerated reactive species (El-Shamy 2020a, 2020b). Among peroxides, the ZnO_2 and MgO_2 are reported for the degradation of organic pollutants (Yang et al. 2017; Zeng et al. 2020). For example, the ZnO_2-based nanocomposite catalyst was used for the photocatalytic degradation of dyes (El-Shamy 2020b). Wu et al. (2019) used MgO_2 nanoparticles to enhanced Fenton-like degradation of organic pollutants. Naim et al. (Al Naim and El-Shamy 2021) also prepared PVA/MgO_2 composite catalyst for organic dye removal. However, there is no report on the preparation of CuAl-LDH/MgO_2 composite catalyst via in-situ growth of MgO_2 on the surface of CuAl-LDH which is used for the degradation of MO dye under dark condition.

In this work, the CuAl-LDH/MgO_2 catalyst was prepared via in-situ growth of MgO_2 on the surface of CuAl-LDH according to the reported literature (Seftel et al. 2014). The characterization for the resulting catalysts was performed and applied in the MO dye degradation. The catalytic efficiency is expected to be active due to the synergistic effects of the LDH and MgO_2. Moreover, the presence of sufficient copper content together with generated H_2O_2 from MgO_2 used for facilitating Fenton-like reaction that could also enhances the MO dye the degradation process. The degradation mechanism was also illustrated in which the LDH initially absorbs pollutants through electrostatic attraction followed by an ion exchanging capability. Then, the hydrogen peroxide generated will be interacted with the adsorbed MO pollutant. Finally, the degradation process will occur through the Fenton-like reaction mechanism. Moreover, the stability of the catalyst was also checked, and it was illustrated that the catalyst was highly stable.

Materials and methods

Chemicals and reagents

All chemicals and reagents were used without further purifications. The $Cu(NO_3)_2{\cdot}3H_2O$, $Al(NO_3)_3{\cdot}9H_2O$, NaOH, Na_2CO_3 (99%), isopropanol ($CH_3CHOHCH_3$) 99.5%), ammonium hydroxide (NH_4OH), $MgCl_2{\cdot}6H_2O$, H_2SO_4, H_2O_2 (30%), methyl orange (MO), ethylene diamine tetra acetic acid disodium salt (Na_2EDTA), and ethanol (C_2H_5OH, 99.9%) were used in the experimental work.

Synthesis of CuAl-LDH catalyst

CuAl LDHs was prepared through co-precipitation method (Zhu et al. 2017). Typically, 15 mmol of Cu $(NO_3)_2{\cdot}3H_2O$ and 7.5 mmol of Al $(NO_3)_2{\cdot}3H_2O$ were dissolved in 100 mL distilled water. The mixture was stirred for 2 h with a molar ratio Cu to Al of 2:1. Under stirring, an aqueous solution of 1.2 M Na_2CO_3 and 0.6 M NaOH were dropped into the salt solution until pH becomes 9. The resulting solution was stirred at room temperature for another 10 h. Finally, the precipitate was separated through filtration and washed with distilled water and ethanol. Finally, the as-synthesized precipitate was dried at 70 °C for 20 h, and CuAl-LDH powder was obtained.

Synthesis of MgO_2

Using the in-situ growth method as reported in the literature (Navik et al. 2017; Lakshmi Prasanna and Vijayaraghavan 2017), 10 mL of H_2O_2 was added to 20 mL of 2 g $MgCl_2{\cdot}6H_2O$ solution and stirred for 2 h at room temperature. Then, 2 M of NaOH was dropped until the white foam was formed and further stirred for 3 h until the foam broken down. The milky white-colored precipitate was aged for 18 h. The precipitate was washed with distilled water, ethanol, and finally with ammonia solution until pH reaches neutral and dried at 100 °C for 2 h.

Synthesis of CuAl-LDH/MgO_2 composites

In a particular method, 0.35 g CuAl-LDH, 0.5 g CuAl-LDH, and 0.65 g CuAl-LDH were added in different beakers containing distilled water and dispersed at room temperature for 30 min to produce homogeneous suspension (Setegn 2020). Then, 2.36 g, 1.81 g, and 1.26 of $MgCl_2{\cdot}6H_2O$ were added into the beakers containing 0.35 g CuAl-LDH, 0.5 g CuAl-LDH, and 0.65 g CuAl-LDH suspension. The suspensions were further stirred for 1 h at room temperature. The pH was adjusted to 12 using NaOH for each suspension. Keeping pH constant, 10 mL of H_2O_2 was dropped to each beaker and stirred for another 4 h. The resulted mixtures were aged at room temperature for 16 h. The obtained precipitates were washed with water and ethanol. Finally, the powders were dried at 100 °C for 2 h and used for the degradation of MO dye. The prepared samples for 0.35, 0.5, and 0.65 g of CuAl-LDH with H_2O_2 were abbreviated as CuAl LDH/MgO_2-35, CuAl-LDH/MgO_2-50, and CuAl-LDH/MgO_2-65, respectively, for simplicity.

Characterization of the catalysts

The X-ray photoelectron spectroscopy (XPS) (ESCALAB 250) was used to determine chemical states of the sample. Shimadzu XRD- 7000 was used to analyze the X-ray diffraction (XRD). The field-emission scanning electron microscopy (FESEM, JSM 6500F, JEOL) and transmitted electron microscopy (TEM) (FEG TEM technai G2 F30) instruments were used for surface characterization. The bonding and functional groups of the samples were checked by using FTIR instrument (Ft/IR-6600 type A). The Shimadzu–3600 Plus UV–Vis spectrophotometer was used to check the concentration of the pollutant.

Catalytic activity test

The degradation of MO was determined by using UV–Vis spectrophotometer. In a particular procedure, 50 mL (10 ppm) MO solution was placed in a beaker. Subsequently, 20 mg of the catalyst was added under neutral conditions at room temperature. Under stirring, 5 mL of the solution was taken in every 20 min interval. After centrifuge, the concentration of MO was determined using UV–Vis spectrometer.

Moreover, the stability of the catalyst was also evaluated by running four cycles. Typically, 200 mg of CuAl-LDH/MgO_2-50 catalyst was added into 500 mL of 10 ppm MO solution. After 100 min, the catalyst was allowed to settle for 2 h. Then, the sample was filtered and re-used for the next remaining runs.

Results and discussion

XRD analysis

Figures 1a–e show the XRD patterns of the MgO_2, CuAl-LDH, and CuAl-LDH/MgO_2 (CuAl-LDH/MgO_2-35, CuAl-LDH/MgO_2-50, CuAl-LDH/MgO_2-65) samples, respectively. As we have seen from the XRD result, all the diffraction patterns of CuAl-LDH/MgO_2 resemble the CuAl-LDH peaks. However, the diffraction peaks of CuAl-LDH/MgO_2-35 get minimum due to the lower content of LDH and the dominant phases of MgO_2 available in catalyst. The typical diffraction peaks at 2θ value of 11.73, 23.59, 32.74, 35.47, 40.22, 47.97, and 60.3° correspond to (300), (006),

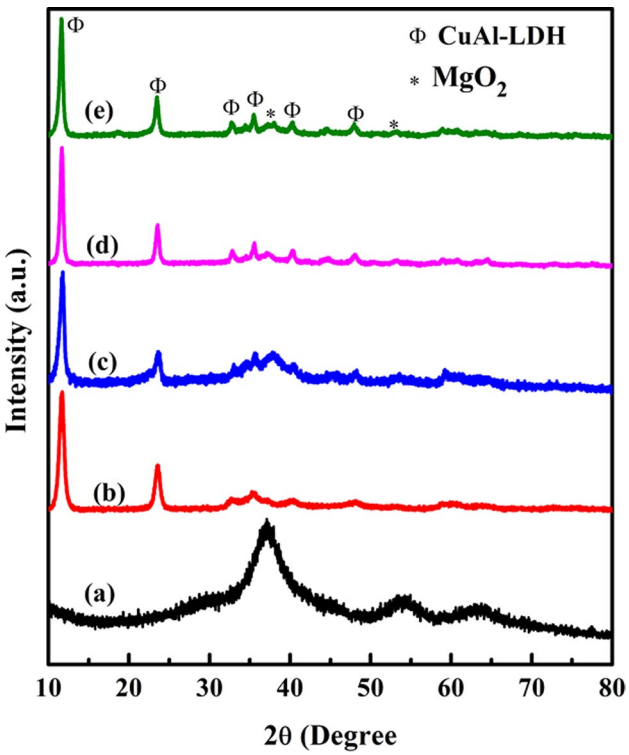

Fig. 1 XRD patterns of **a** MgO_2, **b** CuAl-LDH, **c** CuAl-LDH/MgO_2-35, **d** CuAl-LDH/MgO_2-50, and (e) CuAl-LDH/MgO_2-65

(009), (012), (015), (018), and (110) planes of hydrotalcite-like materials, respectively, (JCPDS card 37-630) (Kameda et al. 2015). The XRD patterns show the formation of the layered double hydroxide which is represented as $Cu_6Al_2(OH)_{16}CO_3{\cdot}4H_2O$. Moreover, the peaks at 11.73° correspond to carbonate (CO_3^{2-}) intercalated in the LDH which is resulted from Na_2CO_3. As it is indicated from Fig. 1a and in all composites, three broad peaks were also obtained at 37.2, 53.4, and 63.4° corresponding to (200), (220), and (311) planes of MgO_2, respectively, (JCPDS No.76-1363) (Wu et al. 2019). The MgO_2 sample was pure, and other extra peaks from MgO and $Mg(OH)_2$ were not observed which is also similar to a reported literature (Wu et al. 2019). The MgO_2 peaks were broader and show smaller crystalline size. The lower crystalline size of magnesium peroxide leads to better dispersion upon forming a composite with the layered double hydroxide. In general, LDHs provide a site to grow magnesium peroxide along with inhibiting irregular growth of MgO_2 with better dispersion.

XPS analysis

The chemical oxidation sate and surface compositions of CuAl-LDH/MgO_2 were confirmed by XPS as shown in Fig. 2. The XPS peaks for Cu $2p_{3/2}$ at 935.88 eV and Cu $2p_{1/2}$ at 956.01 eV demonstrate for $Cu(OH)_2$ (Peng et al. 2018). While the XPS peaks for Cu $2p_{3/2}$ at 933.91 eV and Cu $2p_{1/2}$ at 955.11 eV indicate for Cu^{2+} in the CuO (Zhao et al. 2019). The peak at 77.11 eV binding energy corresponds to the A–O bond (Lu et al. 2017). Moreover, the

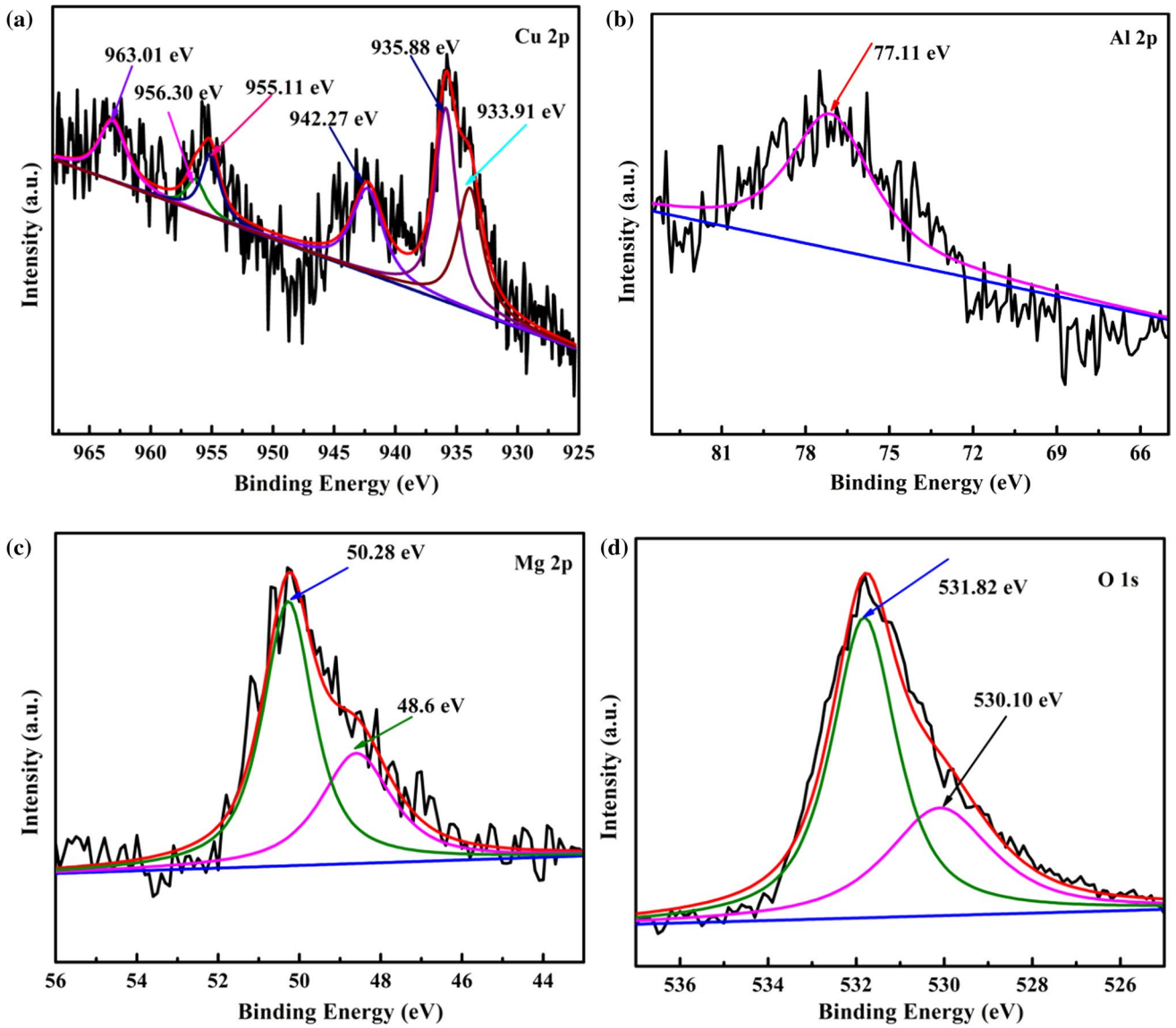

Fig. 2 XPS spectra of **a** Cu 2p, **b** Al 2p, **c**, Mg 2p, and **d** O 1 s for CuAl-LDH/MgO_2-50

binding energies at 50.28 and 48.6 eV indicate the existence of Mg–O and Mg–OH in the sample, respectively (Zeng et al. 2020). The O1s spectrum with binding energy at 531.82 and 530.10 eV is attributed to the lattice oxygen bonded with metals in the composite catalyst (Zeng et al. 2020; Dupin et al. 2000; Almoisheer et al. 2019).

SEM analysis

Figure 3a, b indicates the lower and the higher resolution SEM images of LDH/MgO_2-50 sample, respectively. The sheet-like morphology was observed (Fig. 3a, b). Moreover, the presence of clustered particles growth of MgO_2 was not observed clearly. This is because the MgO_2 particles were immobilized in the presence of CuAl-LDH support. Moreover, the EDS analysis was also used to check the presence of elements like Cu, Al, O, and Mg, in the CuAl-LDH/MgO_2-50 sample as shown in Fig. 3c.

TEM analysis

Figure 4a, d indicates the lower, medium, and higher resolution TEM, and HRTEM images of the CuAl-LDH/MgO_2-50 sample, respectively. The TEM images in Fig. 4a–c exhibit the sheet-like morphology which is similar to SEM images. The resulting nanosheets exhibit the formation of layer structures of CuAl-LDH. Moreover, the TEM also verifies that there was fewer agglomerated porous sheet-like structure for CuAl-LDHs. Additionally, the smaller dot-like particles were shown on the surface of nanosheets. The smaller dot-like morphologies could be MgO_2 nanoparticles. The HRTEM in Fig. 4d also indicates that the CuAl-LDH/MgO_2-50 sample is crystalline.

FTIR analysis

The Fourier transform infrared spectroscopy (FTIR) analysis was also performed as shown in Fig. 5. Figure 5a, b indicates the FTIR spectrum of CuAl-LDH and CuAl-LDH/MgO_2-50

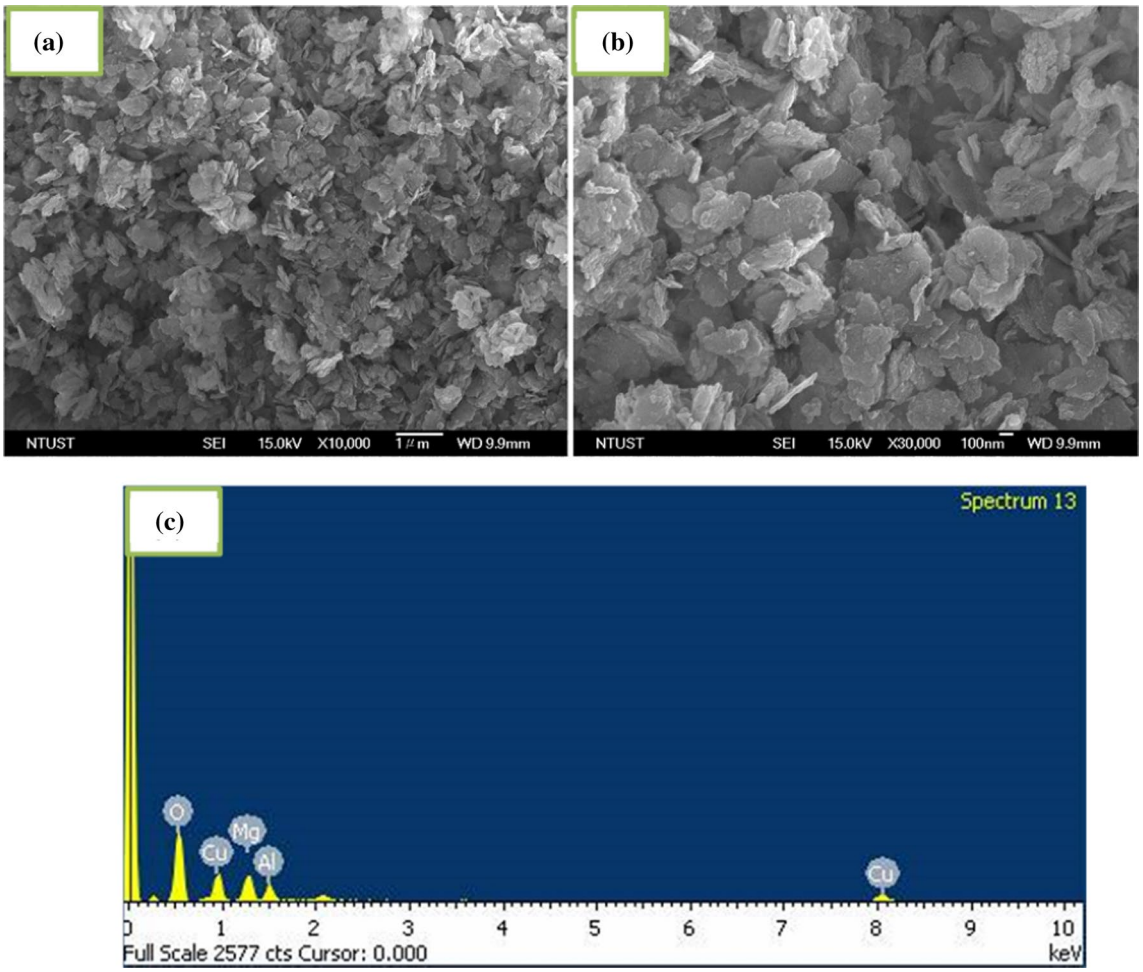

Fig. 3 SEM images of **a**–**b** the lower and the higher resolution, **c** EDS analysis of CuAl-LDH/MgO_2-50 sample

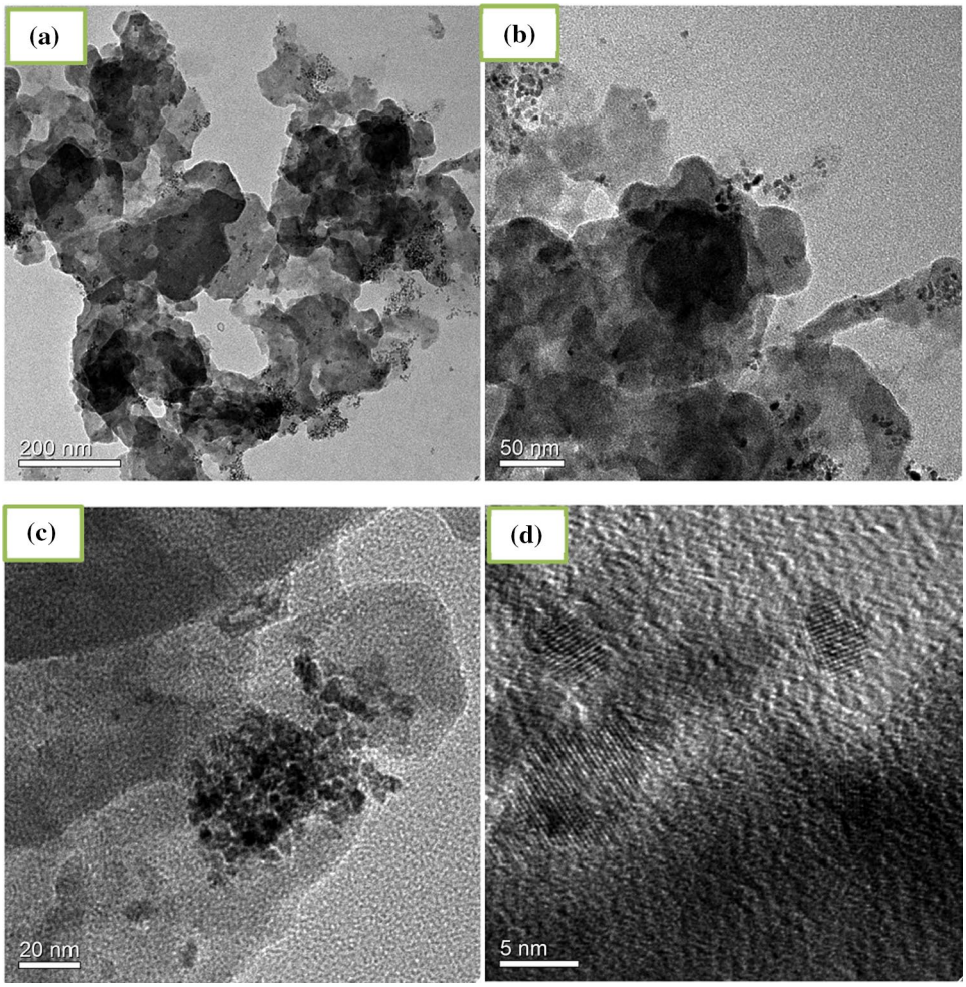

Fig. 4 **a**–**c** the lower, medium, and higher resolution of TEM and **d** HRTEM images of the CuAl-LDH/MgO_2-50 sample

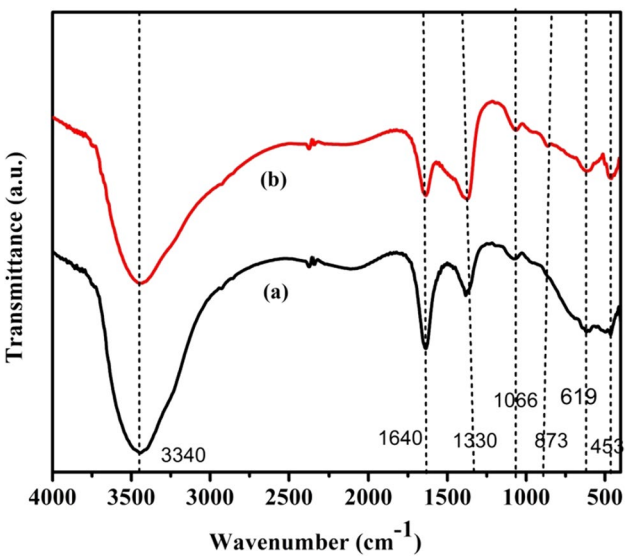

Fig. 5 FTIR spectra of **a** CuAl-LDH, **b** CuAl-LDH/MgO_2-50 samples

samples, respectively. The peak at 3340 and 1640 cm^{-1} attributed to the OH-stretching and the bending modes for the interlayer water and hydroxyls, respectively (Li et al. 2017; Rives et al. 2001). The peak at 1330 cm^{-1} is showed the vibration mode of CO_3^{2-} (Kloprogge et al. 2002). The vibration modes of the carbonate anions were also illustrated at 1066 and 873 cm^{-1} absorption peaks (Li et al. 2017). The 619 and 453 cm^{-1} peaks observed in the sample could be due to lattice vibration of metal oxygen bonding (Rives et al. 2001). In the CuAl-LDH/MgO_2-50 samples (b), the OH stretching is relatively week while CO_3^{2-} vibrations are stronger than its vibration in the LDH sample (a). This is because of the carbonate ion intercalation during MgO_2 deposition onto the LDH.

Nitrogen adsorption–desorption isotherm

The BET analysis of the CuAl-LDH/MgO_2-50 sample indicated in Fig. 6. As it is illustrated in Fig. 6a, the isotherm plot of the CuAl-LDH/MgO_2-50 sample is coincident with the type IV in which it has mesoporous characteristics

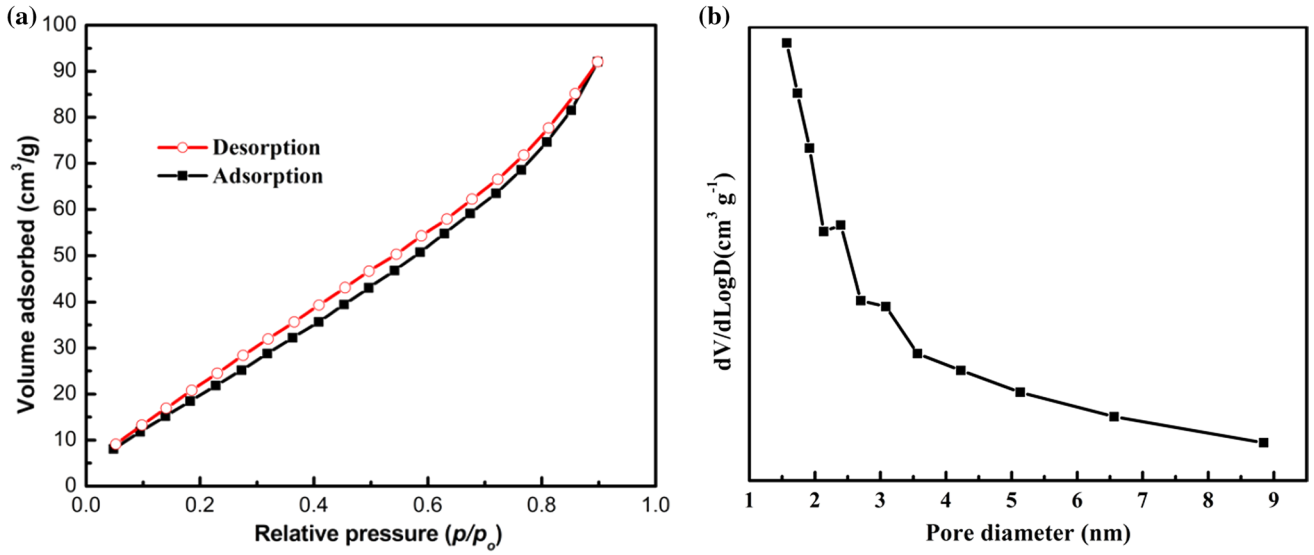

Fig. 6 **a** Nitrogen adsorption and desorption isotherm and **b** the pore size distribution curve of CuAl-LDH/MgO_2-50

(Rouquerol et al. 2013). Moreover, the hysteresis loop demonstrates irregular pore size distribution. The loop can be also defined as H3-type and the pore channels are mainly mesopores (Triantafyllidis et al. 2010). Being H3-type also implying that there is a number of slit shaped pore channels resulted from aggregate or packing of platelet shaped particles of the LDH (Li et al. 2017; Zhi et al. 2010). Figure 6b shows the pore size distribution of the CuAl-LDH/MgO_2-50 sample. From the BET analysis, the total surface area (110.69 m^2/g), pores volume (0.128 cm^2 g^{-1}), and average pore size distribution (1.569 nm) of the sample were also illustrated. The higher surface area of the sample could help to enhance the catalytic activities of CuAl-LDH/MgO_2-50 sample.

Catalytic activity

All the experiments were performed at room temperature under dark condition. The catalytic performance of CuAl-LDH, MgO_2, and CuAl-LDH/MgO_2 composites were measured using UV–visible spectroscopy. The UV–Vis absorption spectra of the MgO_2, CuAl-LDH, CuAl-LDH/MgO_2-35, CuAl-LDH/MgO_2-50, and CuAl-LDH/MgO_2-65 samples are shown in Fig. 7a–e at different interval of times. As it is indicated in Fig. 7a, there was no degradation performance with MgO_2 sample only. MgO_2 cannot generate peroxides to produce active species without other reagents (Lakshmi Prasanna and Vijayaraghavan 2017). Moreover, the CuAl-LDH sample as shown in Fig. 7(b) also had no significant degradation efficiency after it is reached at maximum adsorption capacity within 20 min. On the other hand, the composite form of MgO_2 and CuAl-LDH lead to both adsorption and degradation outcome as shown in Fig. 7c–e Among the composites, CuAl-LDH/MgO_2-35(Fig. 7c) shows a minimum performance. It is due to the minimum amount of copper to produce hydroxyl radicals in the composite catalyst. Among the composites, maximum activity was obtained by CuAl-LDH/MgO_2-50 (Fig. 7d) which had the optimum amount of both CuAl-LDH and MgO_2 in the catalyst system. Further increasing of the CuAl-LDH also deactivates the catalytic activities in which the minimum amount of MgO_2 that can be used to generate active species is available.

The degradation efficiency of the CuAl-LDH/MgO_2-50 composite sample was the highest as shown in Fig. 7d. This particular composition suggests that both copper and MgO_2 are the main components for the generation of optimal active oxygen species. On the other hand, CuAl-LDH/MgO_2-65 composite also showed good performance next to CuAl-LDH/MgO_2-50 composite. The resulting performance could be due to the higher copper content. Initially CuAl-LDH/MgO_2-65 performs well, but as time increases, it doesn't work like CuAl-LDH/MgO_2-50. The reason may be the lowest peroxide generation due to the lower amount of MgO_2 in the LDH/MgO_2-65 composition catalyst. The CuAl-LDH/MgO_2-50 shows an excellent Fenton-like reaction under the neutral condition at which 97% of MO dye was degraded within 100 min. However, CuAl-LDH, MgO_2, CuAl-LDH/MgO_2-35, and CuAl-LDH/MgO_2-65 catalysts degrade only 61, 8, 35, and 69% of MO dye. Generally, the optimum amount of H_2O_2 generated from MgO_2 in aqueous media and the higher content of copper that can able to generate more ROS thereby facilitated the degradation of MO dye. The LDHs also enhance the adsorption of the dye and facilitates for the interaction between the dye and the reactive oxygen species on the surface of the catalyst.

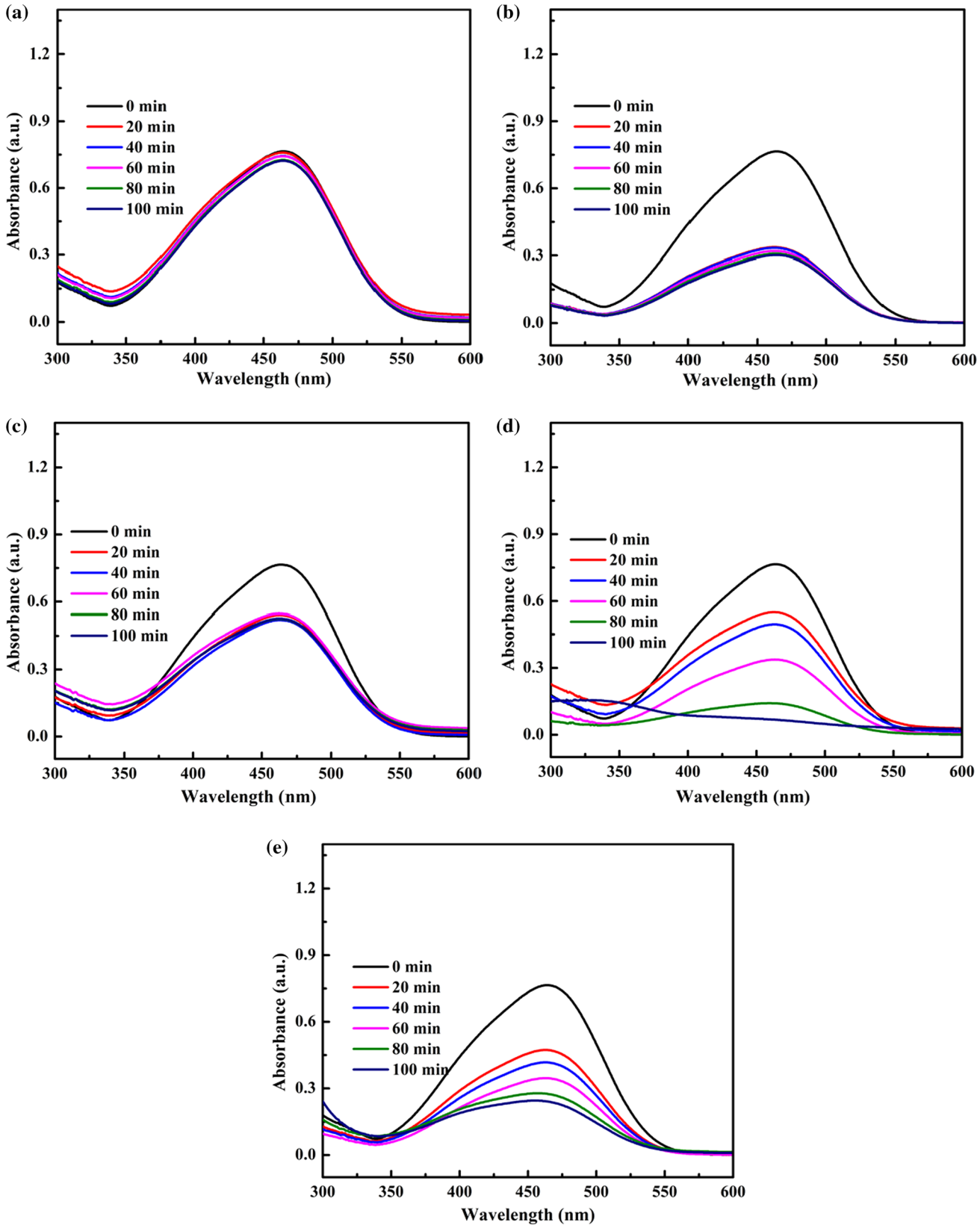

Fig. 7 UV–visible absorption spectra of MO dye with **a** MgO_2, **b** CuAl-LDH, **c** CuAl-LDH/MgO_2-35, **d** CuAl-LDH/MgO_2-50, and **e** CuAl-LDH/MgO_2-65 catalysts

Figure 8b also indicates the degradation kinetics of MO with catalysts at different interval of time fitting with pseudo-first-order reaction and calculated as $-\ln(Ct/Co) = kt$ (where C_0 is initial concentrations, C_t is the concentration after the irradiated time (in a minute), and k is the rate constant (Youssef et al. 2016; Stupar et al. 2020). The rate constant values for the degradations of MO dye with MgO_2, CuAl-LDH, CuAl-LDH/MgO_2-35, CuAl-LDH/MgO_2-50, and CuAl-LDH/MgO_2-65 were 0.0005, 0.0071, 0.0031, 0.031, and 0.011 min-1, respectively. As it is observed from data, the rate constant of the CuAl-LDH/MgO_2-50 catalyst was highest.

Stability test

The stability of the catalyst was also demonstrated and showed in Fig. 9a. It is reported that the difficulty in transporting hydrogen peroxide upon conducting Fenton reaction has been remained as a common challenge. As it is reported, the CuAl-LDH for MO degradation doesn't show persistent activity after multiple runs (Li et al. 2017). In this particular work, the stability of the as synthesized catalyst was relatively higher and stable. As H_2O_2 generated in-situ way, it shows consistent activity for multiple runs. After 4th cycle, the CuAl-LDH/MgO_2-50 catalyst degrades 92.7% of MO dye. Furthermore, the XRD diffiracton patterns after

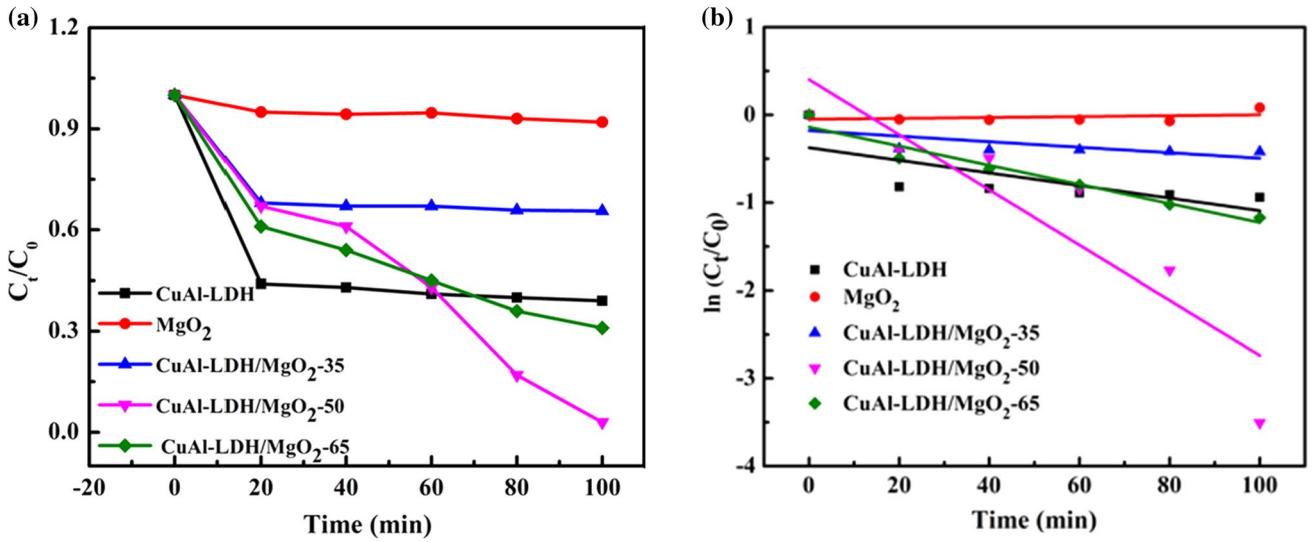

Fig. 8 **a** The C_t/C_o photodegradation results and **b** Pseudo first-order reaction kinetics rates of MO dye with different catalysts

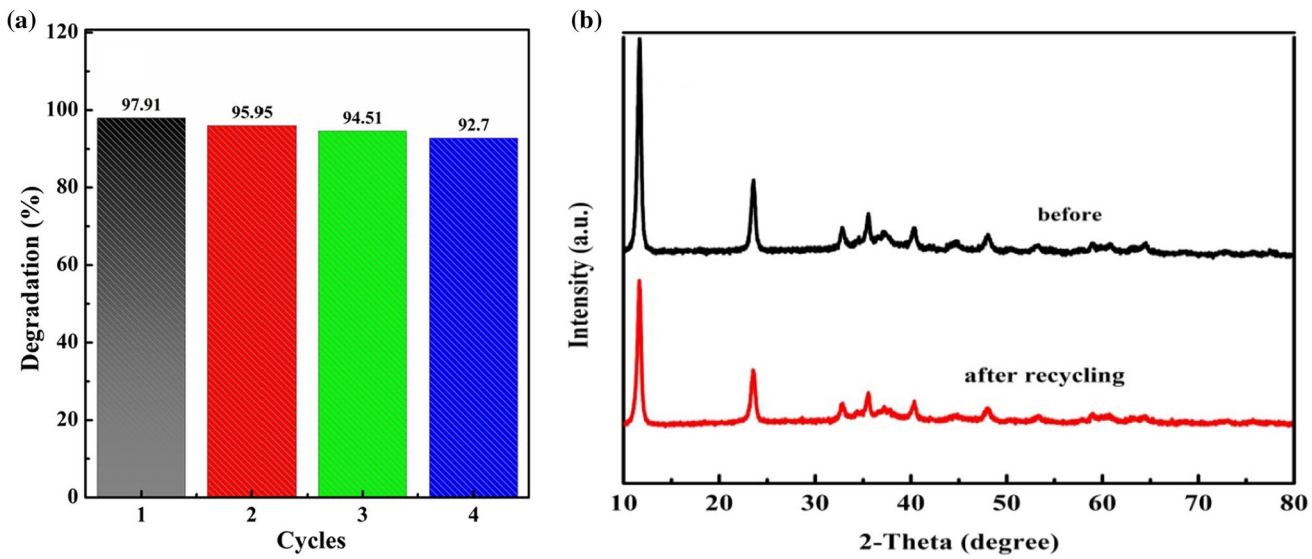

Fig. 9 **a** Re-usability and **b** XRD patterns of CuAl-LDH/MgO_2 -50 catalyst before and after reaction

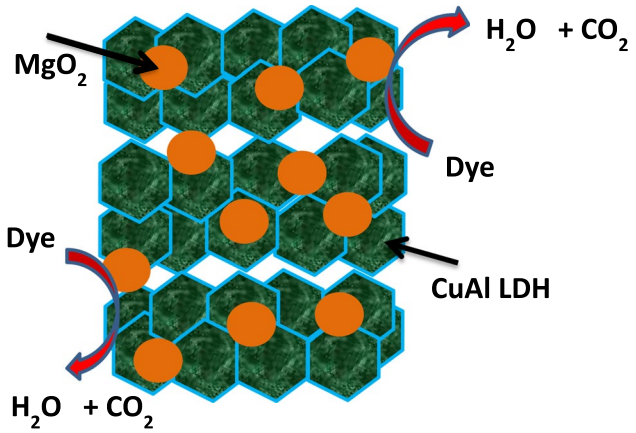

Fig. 10 The degradation mechanism of MO with CuAl-LDH/MgO_2 -50 catalyst

reaction resembles the pattern of the composite before a reaction (Fig. 9b). This further pinpoints the better stability owned by the as-synthesised composite.

Degradation mechanism

Recently, using LDH-based composite catalyst in the water treatment attracts a great attention. The catalytic reaction mechanism was also investigated (Peng et al. 2018). Initially, the organic pollutants will be adsorbed by the catalyst through electrostatic attraction. Under aqueous media magnesium peroxide starts to generate hydrogen peroxide while copper from the hydrotalcite layer converts the generated peroxide into active oxygen species. Once the active species formed, there will be interaction between the reactive oxygen species and MO. Finally, the MO will be converted to CO_2 and H_2O. The generation of ·OH through Fenton-like reaction is dependent on the content of available reagent and peroxide. Figure 10 shows the degradation mechanism of MO with CuAl-LDH/MgO_2 -50 catalyst.

Conclusion

The CuAl-LDH/MgO_2 catalyst was synthesized via in-situ growth of magnesium peroxide on the CuAl-LDH sheet. The catalyst was used for the Fenton-like reaction process. In the reaction process, CuAl-LDH/MgO_2 catalyst had the ability to generate reactive oxygen species under aqueous solution in the dark condition. The CuAl-LDH/MgO_2-50 shows enhanced Fenton-like reaction, and 97% of MO dye was degraded within 100 min. However, CuAl-LDH, MgO_2, CuAl-LDH/MgO_2-35, and CuAl-LDH/MgO_2-65 catalysts degrade only 61, 8, 35, and 69% of MO dye. The LDHs also enhance the adsorption of the dye and facilitates for the interaction between the dye and the reactive oxygen species on the surface of the catalyst. The catalytic enhancement of the composites could be synergistic effects obtained from the CuAl-LDH and MgO_2. Hence, the optimum amount of H_2O_2 generated from MgO_2 in aqueous media and the higher content of copper that can able to generate more ROS thereby facilitating the degradation of MO dye are the main species.

Acknowledgements We would like to acknowledge Adama Science and Technology University (ASTU) for supporting this MSc. thesis work under the grant No. ASTU/SM-R/128/19. We also acknowledged the National Taiwan University of Science and Technology (NTUST) for BET, SEM, TEM, and XPS analysis.

Funding The authors did not receive funds from any funding organization. However, Adama Science and Technology University (ASTU) covered laboratory expenses and other costs for this MSc. student thesis work.

Declarations

Conflict of interest The authors declare no competing interest.

Ethical approval The authors declare no any ethical conduct.

References

Ahmad I, Shoaib Akhtar M, Ahmed E, Ahmad M, Keller V, Qamar Khan W, Khalid NR (2020) Rare earth co-doped ZnO photocatalysts: solution combustion synthesis and environmental applications. Sep Purif Technol 237:116328

Al Naim AF, El-Shamy AG (2021) A new reusable adsorbent of polyvinyl alcohol/magnesium peroxide (PVA/MgO_2) for highly selective adsorption and dye removal. Mater Chem Phys 270:124820

Ali B, Naceur B, Abdelkader E, Karima E, Nourredine B (2020) Competitive adsorption of binary dye from aqueous solutions using calcined layered double hydroxides. Int J Environ Anal Chem. https://doi.org/10.1080/03067319.2020.1766035

Almoisheer N, Alseroury FA, Kumar R, Aslam M, Barakat MA (2019) Adsorption and anion exchange insight of indigo carmine onto CuAl-LDH/SWCNTs nanocomposite: kinetic, thermodynamic and isotherm analysis. RSC Adv 9:560–568

Aragaw SG, Sabir FK, Andoshe DM, Zelekew OA (2020) Green synthesis of p-Co_3O_4/n-ZnO composite catalyst with Eichhornia Crassipes plant extract mediated for methylene blue degradation under visible light irradiation. Mater Res Express 7:095508

Asghar A, Raman AAA, Daud WMAW (2015) Advanced oxidation processes for in-situ production of hydrogen peroxide/hydroxyl radical for textile wastewater treatment: a review. J Clean Prod 87:826–838

Bokare AD, Choi W (2014) Review of iron-free Fenton-like systems for activating H2O2 in advanced oxidation processes. J Hazard Mater 275:121–135

Brillas E, Garcia-Segura S (2020) Benchmarking recent advances and innovative technology approaches of Fenton, photo-Fenton, electro-Fenton, and related processes: a review on the relevance of phenol as model molecule. Sep Purif Technol 237:116337

Cardenas MAR, Ali I, Lai FY, Dawes L, Thier R, Rajapakse J (2016) Removal of micropollutants through a biological wastewater treatment plant in a subtropical climate. Qld-Aust J Environ Health Sci Eng 14:14

Dupin J-C, Gonbeau D, Vinatier P, Levasseur A (2000) Systematic XPS studies of metal oxides, hydroxides and peroxides. Phys Chem Chem Phys 2:1319–1324

Dvininov E, Ignat M, Barvinschi P, Smithers M, Popovici E (2010) New SnO_2/MgAl-layered double hydroxide composites as photocatalysts for cationic dyes bleaching. J Hazard Mater 177:150–158

El-Shamy AG (2020) Synthesis of new magnesium peroxide (MgO_2) nano-rods for pollutant dye removal and antibacterial applications. Mater Chem Phys 243:122640

El-Shamy AG (2020) New carbon quantum dots nano-particles decorated zinc peroxide (Cdots/ZnO_2) nano-composite with superior photocatalytic efficiency for removal of different dyes under UV-A light. Syn Metals 267:116472

Fei W, Song Y, Li N, Chen D, Xu Q, Li H, He J, Lu J (2019) Fabrication of visible-light-active ZnO/ZnFe-LDH heterojunction on Ni foam for pollutants removal with enhanced photoelectrocatalytic performance. Sol Energy 188:593–602

Gao Z, Liang J, Yao J, Zhao Y, Meng Q, He G, Chen H (2021) Synthesis of Ce-doped NiAl LDH/RGO composite as an efficient photocatalyst for photocatalytic degradation of ciprofloxacin. J Environ Chem Eng 9:105405

Garcia-Muñoz P, Fresno F, Lefevre C, Robert D, Keller N (2020) Synergy effect between photocatalysis and heterogeneous photo-Fenton catalysis on Ti-doped $LaFeO_3$ perovskite for high efficiency light-assisted water treatment, Catalysis. Sci Technol 10:1299–1310

Hadjltaief HB, Bairq ZAS, Shi C, Benzina M (2021) Evaluation of sono-assisted solar/Fenton process for indigo carmine degradation over magnetic ZnO-Fe_3O_4 supported Tunisian kaolinite clay. Surf Interfaces 26:101395

Kameda T, Uchiyama T, Yoshioka T (2015) Cu–Al layered double hydroxides intercalated with 1-naphthol-3, 8-disulfonate and dodecyl sulfate: adsorption of substituted phenols from aqueous media. New J Chem 39:6315–6322

Khataee A, Sadeghi Rad T, Nikzat S, Hassani A, Aslan MH, Kobya M, Demirbaş E (2019) Fabrication of NiFe layered double hydroxide/reduced graphene oxide (NiFe-LDH/rGO) nanocomposite with enhanced sonophotocatalytic activity for the degradation of moxifloxacin. Chem Eng J 375:122102

Kloprogge JT, Wharton D, Hickey L, Frost RL (2002) Infrared and Raman study of interlayer anions CO_3^{2-}, NO_3^-, SO_4^{2-} and ClO_4^- in Mg/Al-hydrotalcite. Am Miner 87:623–629

Lakshmi Prasanna V, Vijayaraghavan R (2017) Simultaneous Fenton–photocatalytic reactions through a new single catalyst (Nano ZnO_2/Fe^{2+}) for dye degradation. J Phys Chem C 121:18557–18563

Lestari PR, Takei T, Kumada N (2021) Novel ZnTi/C_3N_4/Ag LDH heterojunction composite for efficient photocatalytic phenol degradation. J Solid State Chem 294:121858

Li J, Zhang S, Chen Y, Liu T, Liu C, Zhang X, Yi M, Chu Z, Han X (2017) A novel three-dimensional hierarchical CuAl layered double hydroxide with excellent catalytic activity for degradation of methyl orange. RSC Adv 7:29051–29057

Lu H, Zhu Z, Zhang H, Zhu J, Qiu Y, Zhu L, Küppers S (2016) Fenton-like catalysis and oxidation/adsorption performances of acetaminophen and arsenic pollutants in water on a multimetal Cu–Zn–Fe-LDH. ACS Appl Mater Interfaces 8:25343–25352

Lu W, Iwasa Y, Ou Y, Jinno D, Kamiyama S, Petersen PM, Ou H (2017) Effective optimization of surface passivation on porous silicon carbide using atomic layer deposited Al_2O_3. RSC Adv 7:8090–8097

Lu D, Zelekew OA, Abay AK, Huang Q, Chen X, Zheng Y (2019) Synthesis and photocatalytic activities of a CuO/TiO_2 composite catalyst using aquatic plants with accumulated copper as a template. RSC Adv 9:2018–2025

Ma J, Jia N, Shen C, Liu W, Wen Y (2019) Stable cuprous active sites in Cu^+-graphitic carbon nitride: structure analysis and performance in Fenton-like reactions. J Hazard Mater 378:120782

Marinho BA, Cristóvão RO, Djellabi R, Loureiro JM, Boaventura RAR, Vilar VJP (2017) Photocatalytic reduction of Cr(VI) over TiO_2-coated cellulose acetate monolithic structures using solar light. Appl Catal B 203:18–30

Mustapha S, Ndamitso M, Abdulkareem A, Tijani J, Shuaib D, Ajala A, Mohammed A (2020) Application of TiO_2 and ZnO nanoparticles immobilized on clay in wastewater treatment: a review, Applied Water. Science 10:1–36

Navik R, Thirugnanasampanthan L, Venkatesan H, Kamruzzaman M, Shafiq F, Cai Y (2017) Synthesis and application of magnesium peroxide on cotton fabric for antibacterial properties. Cellulose 24:3573–3587

Opoku F, Kiarii EM, Govender PP, Mamo MA (2017) Metal oxide polymer nanocomposites in water treatments. In: Akitsu T (ed) Descriptive inorganic chemistry researches of metal compounds. IntechOpen, London

Peng X, Wang M, Hu F, Qiu F, Zhang T, Dai H, Cao Z (2018) Multipath fabrication of hierarchical CuAl layered double hydroxide/carbon fiber composites for the degradation of ammonia nitrogen. J Environ Manage 220:173–182

Rives V, Dubey A, Kannan S (2001) Synthesis, characterization and catalytic hydroxylation of phenol over CuCoAl ternary hydrotalcites. Phys Chem Chem Phys 3:4826–4836

Rouquerol J, Rouquerol F, Llewellyn P, Maurin G, Sing KS (2013) Adsorption by powders and porous solids: principles, methodology and applications. Academic press, London

Rupa EJ, Anandapadmanaban G, Chokkalingam M, Li JF, Markus J, Soshnikova V, Perez ZEJ, Yang D-C (2019) Cationic and anionic dye degradation activity of Zinc oxide nanoparticles from Hippophae rhamnoides leaves as potential water treatment resource. Optik 181:1091–1098

Seftel E, Puscasu M, Mertens M, Cool P, Carja G (2014) Assemblies of nanoparticles of CeO_2–ZnTi-LDHs and their derived mixed oxides as novel photocatalytic systems for phenol degradation. Appl Catal B 150:157–166

Setegn G (2020) Degradation of methyl orange by fenton reaction using CuAl layered double hydroxide/MgO_2 Composite Catalyst under Dark Condition, Thesis, ASTU.

Soltani RDC, Jorfi S, Ramezani H, Purfadakari S (2016) Ultrasonically induced ZnO–biosilica nanocomposite for degradation of a textile dye in aqueous phase. Ultrason Sonochem 28:69–78

Soltani R, Pelalak R, Pishnamazi M, Marjani A, Shirazian S (2021) A water-stable functionalized NiCo-LDH/MOF nanocomposite: green synthesis, characterization, and its environmental application for heavy metals adsorption. Arabian J Chem 14:103052

Stupar SL, Grgur BN, Radišić MM, Onjia AE, Ivanković ND, Tomašević AV, Mijin DŽ (2020) Oxidative degradation of Acid Blue 111 by electro-assisted Fenton process. J Water Process Eng 36:101394

Torres-Pinto A, Sampaio MJ, Teixo J, Silva CG, Faria JL, Silva AM (2020) Photo-Fenton degradation assisted by in situ generation of hydrogen peroxide using a carbon nitride photocatalyst. J Water Process Eng 37:101467

Triantafyllidis KS, Peleka EN, Komvokis VG, Mavros PP (2010) Iron-modified hydrotalcite-like materials as highly efficient phosphate sorbents. J Colloid Interface Sci 342:427–436

Wan Y, Wang J, Huang F, Xue Y, Cai N, Liu J, Chen W, Yu F (2018) Synergistic effect of adsorption coupled with catalysis based on graphene-supported MOF hybrid aerogel for promoted removal of dyes. RSC Adv 8:34552–34559

Wu D, Bai Y, Wang W, Xia H, Tan F, Zhang S, Su B, Wang X, Qiao X, Wong PK (2019) Highly pure MgO_2 nanoparticles as robust solid oxidant for enhanced Fenton-like degradation of organic contaminants. J Hazard Mater 374:319–328

Yang D, Gondal MA, Yamani ZH, Baig U, Qiao X, Liu G, Xu Q, Xiang D, Mao J, Shen K (2017) 532nm nanosecond pulse laser triggered synthesis of ZnO_2 nanoparticles via a fast ablation technique in liquid and their photocatalytic performance. Mater Sci Semicond Process 57:124–131

Youssef NA, Shaban SA, Ibrahim FA, Mahmoud AS (2016) Degradation of methyl orange using Fenton catalytic reaction. Egypt J Pet 25:317–321

Zelekew OA, Kuo D-H (2017a) Synthesis of a hierarchical structured NiO/NiS composite catalyst for reduction of 4-nitrophenol and organic dyes. RSC Adv 7:4353–4362

Zelekew OA, Kuo D-H (2017b) Facile synthesis of SiO_2@CuxO@ TiO_2 heterostructures for catalytic reductions of 4-nitrophenol and 2-nitroaniline organic pollutants. Appl Surf Sci 393:110–118

Zelekew OA, Kuo D-H, Yassin JM, Ahmed KE, Abdullah H (2017) Synthesis of efficient silica supported TiO_2/Ag_2O heterostructured catalyst with enhanced photocatalytic performance. Appl Surf Sci 410:454–463

Zelekew OA, Aragaw SG, Sabir FK, Andoshe DM, Duma AD, Kuo D-H, Chen X, Desissa TD, Tesfamariam BB, Feyisa GB, Abdullah H, Bekele ET, Aga FG (2021) Green synthesis of Co-doped ZnO via the accumulation of cobalt ion onto Eichhornia crassipes plant tissue and the photocatalytic degradation efficiency under visible light. Mater Res Express 8:025010

Zeng W, Yin Z, Gao M, Wang X, Feng J, Ren Y, Wei T, Fan Z (2020) In-situ growth of magnesium peroxide on the edge of magnesium oxide nanosheets: ultrahigh photocatalytic efficiency based on synergistic catalysis. J Colloid Interface Sci 561:257–264

Zhang H, Li G, Deng L, Zeng H, Shi Z (2019) Heterogeneous activation of hydrogen peroxide by cysteine intercalated layered double hydroxide for degradation of organic pollutants: Performance and mechanism. J Colloid Interface Sci 543:183–191

Zhang Y, Zhang C, Zhou Z, Wu Y, Xing S (2021) Degradation of ciprofloxacin by persulfate activation with CuO supported on Mg Al layered double hydroxide. J Environ Chem Eng 9:106178

Zhao F, Fan L, Xu K, Hua D, Zhan G, Zhou S-F (2019) Hierarchical sheet-like Cu/Zn/Al nanocatalysts derived from LDH/MOF composites for CO_2 hydrogenation to methanol. J CO2 Util 33:222–232

Zhi Y, Li Y, Zhang Q, Wang H (2010) ZnO nanoparticles immobilized on flaky layered double hydroxides as photocatalysts with enhanced adsorptivity for removal of acid red G. Langmuir 26:15546–15553

Zhu Y, Rong J, Zhang T, Xu J, Dai Y, Qiu F (2017) Facile and controlled fabrication of Cu–Al layered double hydroxide nanosheets/laccase hybrid films: a route to efficient biocatalytic removal of congo red from aqueous solutions. ACS Appl Nano Mater 1:284–292